Anneliese Hagl[1]

Durability by Design: New Results on Load Carrying Silicone Bonding

---

Reference: Hagl, A., **"Durability by Design: New Results on Load Carrying Silicone Bonding,"** *Third Symposium on Durability of Building and Construction Sealants and Adhesives, Denver CO, June 25-26, 2008*

Abstract: In the year 2000, the Herz-Jesu church was finalized featuring a glass façade with very advanced bonded load carrying structures. The façade was stiffened in such a way that wind and dead loaded glass elements were joined to stainless steel channels by a two-component Silicone adhesive for load transfer. Durability aspects related to the applied type of bonding were already presented by the author during the "Fourth International Symposium on Durability of Building and Construction Sealants and Adhesives" in the year 2003.

The technological questions raised by the design of the Herz-Jesu church initiated detailed research investigations in Germany concerning complex bonding geometries for civil engineering purposes. The studies comprised experimental and theoretical activities dedicated to the mechanical properties of two-component Silicone adhesives as well as to the behavior of additional bonding geometries such as L- and T-type steel elements.

In the context of these research activities, focus was given to different aspects directly or indirectly related to durability issues. Regarding adhesive material behavior, tension, compression and shear tests were performed under aged and unaged conditions for analyzing the impact of an aggressive environment. Concerning load carrying capacities and failure mechanisms of the different bonding geometries, several degradation modes were introduced to the specimens in a systematic manner allowing to assess the behavior in the view of partial failure.

This paper presents an overview of the obtained experimental results complemented by detailed Finite Element Analysis. Results shown for the U-type bonding geometry are reviewed in the light of new experimental results. Furthermore the T-type bonding geometry is assessed in a similar way as already done for the U-type bonding geometry. Finally, the paper concludes by directly comparing all investigated bonding geometries in the view of durability aspects.

Keywords: Structural glazing, bonding design, durability design, joint geometry, FE analysis

---

[1] Managing Director, A. Hagl Ingenieurgesellschaft mbH, Munich, Bodenseestr. 217, D-81243 Munich, Germany, email: a.hagl-ingenieure@t-online.de, www.a-hagl-ingenieure.de

Nomenclature

BSL	Baseline
ETAG	European Technical Approval Guideline
FRD	Front region disabled
L_f	Length of flange
PFC	Parallel flange channel
SRD	Side region disabled

Introduction

Beyond architectural highlights – clearly visible in Figure 1 – the Herz Jesu church in Munich, Germany, offers also highly sophisticated solutions from civil engineering point of view. One major advanced topic related to the glass façade is the extensive application of load bearing U-type bonding based on a two-component Silicone structural adhesive. The bonding combines horizontal and vertical glass beams with attachment points providing load transfer in order to ensure structural integrity of the entire glass façade, see Figure 2. For details of this special design, the reader is referred to Refs. [1, 2].

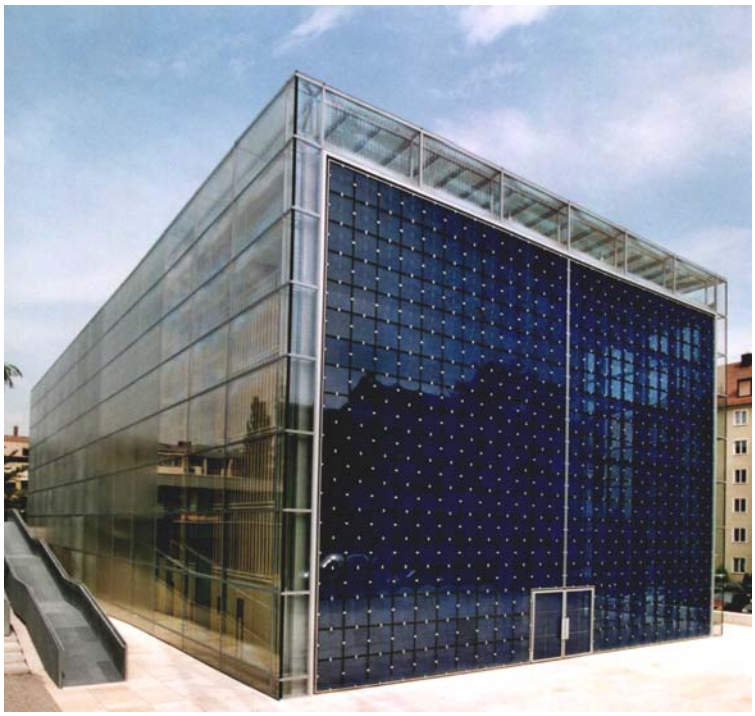

Figure 1 – *Glass façade of Herz Jesu church, Munich*

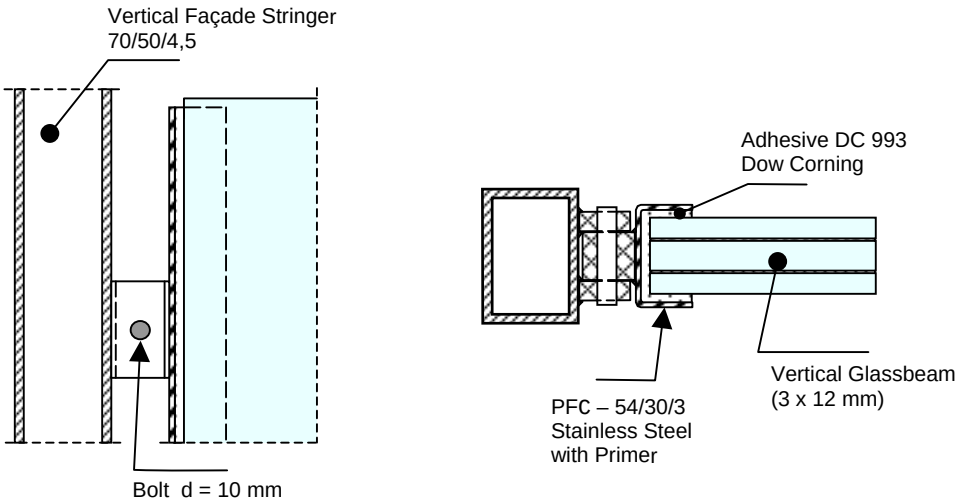

Figure 2 – *Bonding design – glass façade Herz Jesu church*

The horizontal glass beams are foreseen to mainly counteract wind loads acting on the façade of areas 47.04 m by 16.00 m (154.3 ft by 52.5 ft) in longitudinal direction and 19.00 m by 16.00 m (62.3 ft by 52.5 ft) in lateral direction of the building. The nature of these wind loads is stochastic in time depending on the local environmental conditions. The wind loads are typically considered as quasi-steady loads i.e. inertia effects of the façade structure are small compared to other load sources which is e.g. in contrast to bomb blast situations. A wind load sizing hypothesis based on German regulations had to be taken into account regarding the required strength of the structural bonding.

The main function of the vertical glass beams consists in keeping the horizontal glass beams in position in order to allow them to transfer the wind loads to the façade framework. The nature of the related loads is mainly dictated by dead loads of both horizontal and vertical glass beams i.e. constant loads over all times acting on the structural bonding as well. Thus, for designing and sizing of the structural bonding, creep was a topic to be accordingly anticipated.

The Herz Jesu church building was finalized in 2000. Although inspected regularly in detail, neither global nor local defectives related to the structural bonding were observed until today, see Figure 3. In contrast minor optical deficiencies have been noted in terms of material incompatibility and cracks with respect to locally applied hard sealing material, Figure 3 bottom right.

In Ref. [2], durability aspects of structural bonding geometries as applied to the glass facade of the Herz Jesu church were discussed in detail. Table 1 which is mainly based on the outcome of Ref. [3] gives an overview of major important topics for joint durability.

In the view of the glass façade design process or in the view of more general building design processes, some of these key topics can be favorably taken in consideration while others might be determined by requirements outside of the durability aspect.

Figure 3 –*Glass façade in the year 2008*

Environment	Arrangement of bonded structures inside glass façade being favorable regarding humidity, temperature
Adhesive type	Selection of Silicone adhesive dominated by structural glazing requirements
Adherents	Glass beams resulting from façade design, stainless steel channels selected for reduced corrosion
Adherent surface pre-treatment	Purification of glass surfaces by a special cleaning agent, additional coating of channel surfaces with primer
Moisture / Stress / Temperature	Effects of moisture, stress and temperature mainly determined by bonding geometry: careful bonding design required

Table 1 – *Parameters affecting joint durability*

Taking into account the table presented above, this paper is intended to mainly address issues regarding joint design and stress distributions. These areas of interest are accompanied by some experimental results aiming on baseline physical properties of the two-component Silicone adhesive. The conclusions can be mapped to other adhesives in case they fulfill the following two conditions: They show a certain level of incompressibility for example all elastomerics and the adhesive bonding layer has a comparable thickness. The main objective of this paper is to extend the knowledge of the fully functional U-type bonding to degraded bonding configurations on the one hand and to other geometries such as T-type, L-type and E-type bonding geometries on the other hand. The paper starts with some adhesive material test results in the next

section in order to provide a foundation for experimental and numerical results afterwards.

Adhesive Material Test Results

Although Silicone adhesives differ from a chemical point of view from other elastomerics regarding their anorganic Si-O backbone they share a lot of mechanical pecularities with – chemically speaking – more conventional elastomerics like rubber. Such characteristics are e.g. large elastic deformations known as hyperelasticity, Mullins effect, almost perfect incompressibility, non-viscous damping behavior, etc. An adequate comprehensive description of this complex mechanical behavior of elastomerics for general applications is still the aim of extensive research activities around the world and is out of the scope of this paper. Nevertheless, appropriate assumptions and approximations allow to beneficially use today's knowledge by accordingly reducing the required complexity of material description for civil engineering purposes. In the view of the glass façade, wind and dead loads are main parameters for sizing which allow for a quasi-steady material modeling thus skipping time depending phenomena such as visco-elasticity. Furthermore, it is assumed that the critical load cases are not governed by a cyclic loading scheme with already experienced stress states in order to neglect the Mullins effect. As result of these approximations, representative material tests on the one hand can be reduced to quasi-steady load tests. On the other hand, hyperelastic material laws available in commercial FE codes such as Mooney-Rivlin, Ogden, etc. can be applied favorably for related numerical investigations.

Figure 4 shows the results of a tension test comparing aged with unaged specimens of baseline bone type. The "aged" specimens were exposed to artificial aging according to the following procedure [4]:

• 3 days	80° C temperature	
• 10 days	45° C temperature	de-mineralized water with cleaning agent (5%)
• 3 days	80° C temperature	
• 10 days	45° C temperature	de-mineralized water, UV radiation 50 +/-5 W/m^2
• 1 day	23° C temperature	baseline laboratory conditions
• 8 days	45° C temperature	salted water (50 g salt/l), UV radiation 50 +/- 5 W/m^2
• 2 days	-30° C temperature	
• 1 day	23° C temperature	test performance

With respect to the experimental results shown in Figure 4, the strength of the specimens was obviously not affected by this procedure but a modification in the elastic behavior – i.e. effective stiffness and flexibility – is visible. The aged specimens show a somewhat softer behavior.

A similar test comparing aged and unaged behavior was performed with shear specimens. The same procedure as presented above for the tension tests was applied

to the specimens for artificial aging. Figure 5 shows the experimental results confirming the observations that aging leads to lower stiffness or higher flexibility respectively. In opposite to the tension tests the maximum load of the aged specimen is slightly reduced compared to the unaged counterpart. Nevertheless – as it will be shown later – the importance of shear strength is lower than the importance of tension strength for the investigated bonding geometries when undamaged.

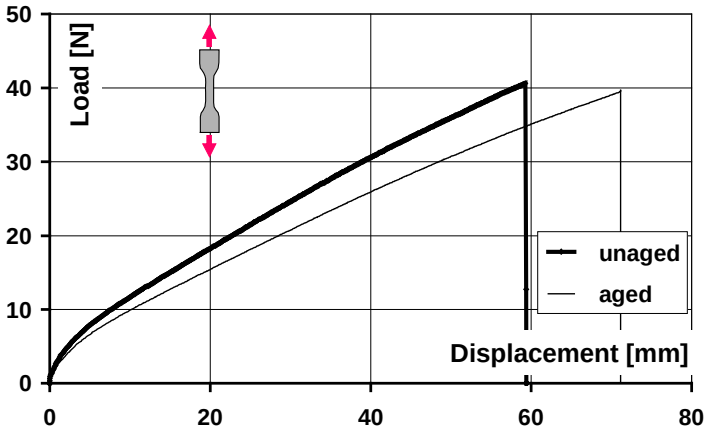

Figure 4 – *Comparison of tension tests – aged versus unaged [4]*

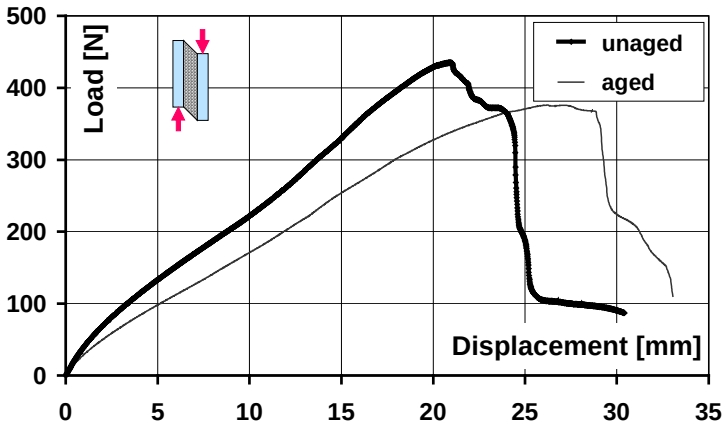

Figure 5 – *Comparison of shear tests – aged versus unaged [4]*

The presented results are related to a baseline test environment under laboratory conditions at 23° C for both unaged and aged specimens. Tension and shear tests were performed in addition at high and low temperatures in order to study the impact of temperature on strength. Figure 6 demonstrates the impact of temperature on tension tests. Regarding strength, a clear trend is visible with lower temperatures related to higher maximum loads and vice versa. Regarding elastic behavior, a unique trend is not visible for the three temperature levels investigated. While stiffness are very similar for medium and high temperatures, the test at low temperature shows a significantly higher stiffness.

In Figure 7, one can see corresponding results for shear loading. Regarding strength, the trend of increasing maximum loads for decreasing temperatures – already

identified by the tension test results – is confirmed. Regarding the elastic behavior, similar stiffness is obtained for all investigated temperature levels. Figures 8 and 9 present a compilation of all results including additional statistical information for both tension and shear.

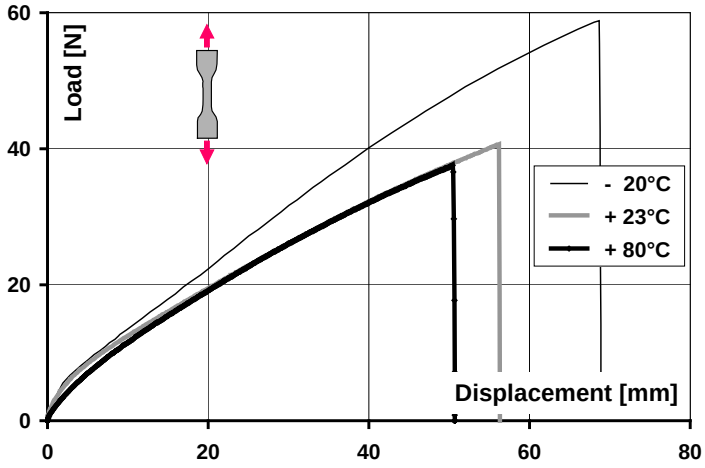

Figure 6 – *Comparison of tension tests – different temperatures [4]*

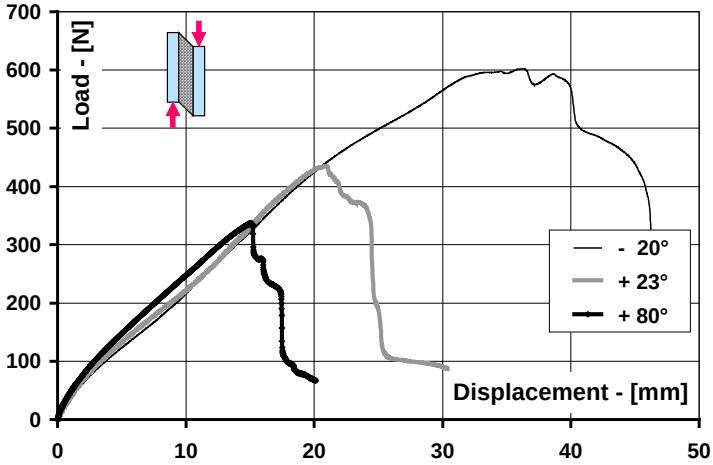

Figure 7 – *Comparison of shear tests – different temperatures [4]*

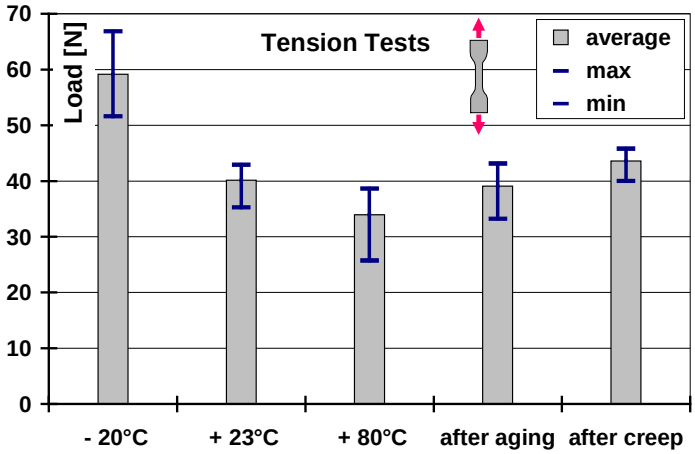

Figure 8 – *Overview of tension test results*

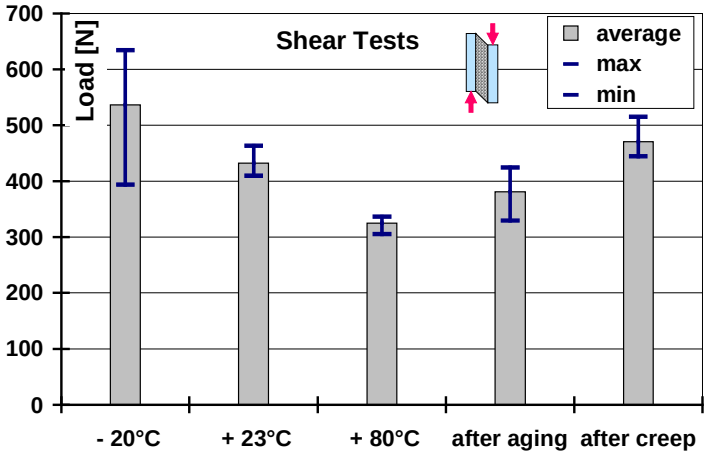

Figure 9 – *Overview of shear test results*

In addition creep tests were performed in the frame of the tension test campaign. Figure 10 compares results of regular specimens with those exposed to creep before. Creep was tested by a tension loading equivalent to 20% of maximum strain for a duration of 105 days. As it can be clearly identified in the figure, there is a similar behavior of both specimens concerning stiffness and maximum loads in the highly loaded regime. At least for the tested conditions there is obviously only limited impact of creep on the highly loaded adhesive facilitating the consideration of creep in the design process significantly.

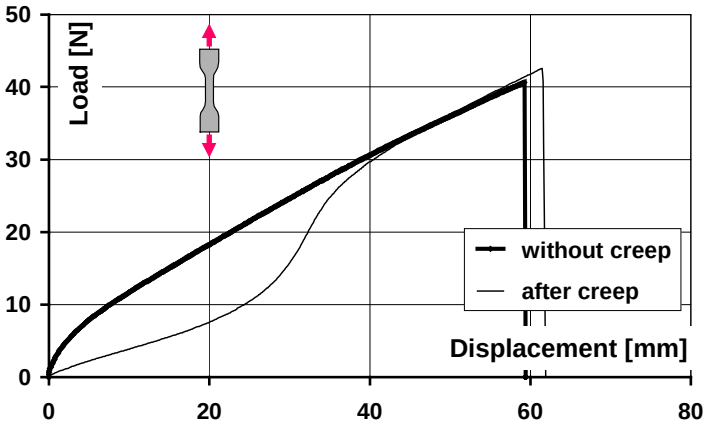

Figure 10 – *Comparison of tension tests – without and after creep [4]*

Concluding the outcome of the test campaign the experimental results presented above build a database allowing to assess the impact of various environmental parameters on joint strength for civil engineering purposes. Special importance for the aim of this paper has the determination of the impact of aging on maximum loads showing almost no effects on tension specimens and a minor degradation for shear specimens. Compression tests are of low interest because on the one hand elastomerics are assumed not to fail under pure compression loads and on the other hand it is difficult to design appropriate compression tests without running into problems with respect to buckling and friction. For future applications other test parameters might be of interest as well such as high speed loading for analysis of bomb blast etc.

U-type Bonding Geometries without and with Degradation

Since the beginning of the application of the U-type bonding geometry, focus was given on physical insight of the failure mechanisms behind under tension loading. Recalling Table 1, one key element for joint durability is joint stress; thus knowledge of stress and related failure is also important for assessing durability aspects of the joint design. Other load cases are less critical because either they are simpler to understand or they are less important regarding strength issues. Shear loading is an example for easier physical understanding. In the case of shearing the glass components relative to the steel framework, simple shear assumptions for each part of the bonding allow to estimate stiffness and strength of the bonding with adequate accuracy by comparing the design values of shear stress and shear strain versus shear test data e.g. of ETAG specimens. The case of compression loading of the bonding is an example for a less critical case concerning strength issues. In this case, the main load path is established by compression of the adhesives. Based on engineering practice it is widely accepted that elastomerics do not fail under high compression loads experienced under conventional civil engineering applications.

Processing the specimen test results of the U-type bonding geometry of the Herz Jesu church, significant differences were observed compared to H-type ETAG specimens under tension loads. Based on theoretical and numerical test results it was hypothesized that the specimens of the U-type bonding fail in two steps [1, 4] which can be explained by the fact that front and side regions of the U-type bonding are acting in different manners. Numerical predictions revealed a highly stressed front region partly evoked by the almost perfect incompressibility of the applied Silicone adhesives. Due to the surrounding relatively stiff components such as the glass body or the steel channels and the small share of free surface of the adhesive the hereby suppressed lateral contraction of the Silicone leads to high efficient stiffness in tension and thus to high stress levels introducing material damage with increasing loading mainly in the front region quite soon. The impact of this mechanism is identified as a significant drop of stiffness in the experimental results. In the next stage, loads are shifted from the front region to the side region until the side regions finally fail due to shear strength limits.

In the meantime this hypothesis was experimentally investigated by the analysis of degraded U-type bonding geometries as presented in [5]. Degradation was introduced by preventing the adhesion due to a PE-foil inserted. Two types of degradation were studied: one with side regions disabled (SRD) and one with front region disabled (FRD), see Figure 11. Figure 12 shows experimental results comparing the fully operational bonding (BSL) with degradations at side and front regions. In a first glance, the behavior of the BSL configuration can be understood as a superposition of the SRD and FRD configurations. The dominant role of the front region for small displacements is clearly visible comparing the BSL case with the SRD case both featuring a fully operative front region at the beginning and showing high initial stiffness. The behavior at large displacements is easily identified as dominated by shear comparing the BSL case with the FRD case. Concluding these results, the hypothesis of failure beginning at the front region and finally propagated towards the side regions is clearly confirmed by these experiments.

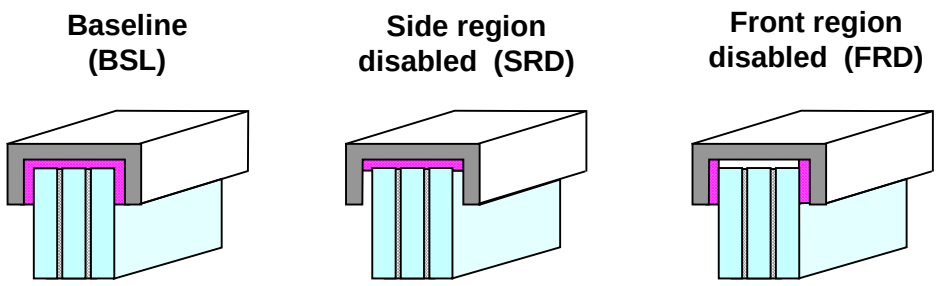

Figure 11 – *U-type bonding test figurations*

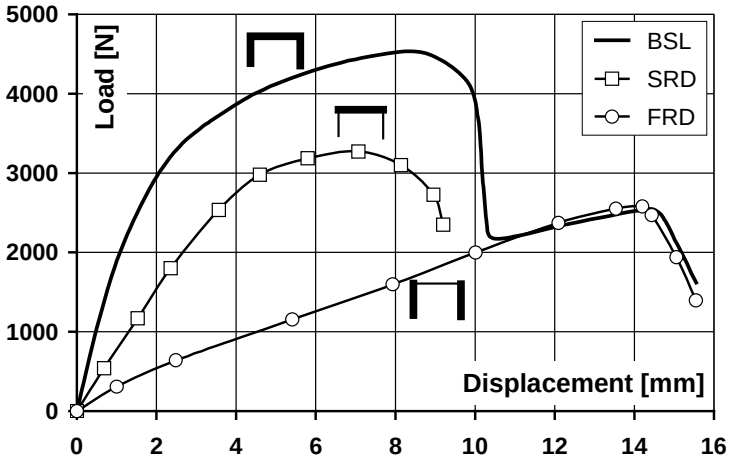

Figure 12 – *U-type bonding geometry – test results*

What are the consequences of these findings regarding design, strength and durability ? First, the failure mechanism in two steps can be tailored for a dedicated safety concept of the bonding. It is desirable that after experiencing an overload condition, bonding strength is not totally lost still preserving a certain amount of mechanical integrity until repair. A safety concept might be based on the natural activation of the side regions in case of the front region being lost due to overload. This approach leads to design rules for the sizing of the side regions depending on the required strength levels after overload. Second, the side regions also lead to the encapsulation of highly loaded adhesive regions at the front of the U-type bonding which is favorable under durability aspects. Here, the geometry of the side regions affects stress levels on free surfaces on the one hand and diffusion of aggressive environmental media into the adhesive on the other hand.

In order to assess the loading of the side region and the related impact on durability, stress distributions of U-type bonding geometries have been investigated using Finite Element analysis. Maximum principal stresses are considered as representative stress level indicators for the Silicone adhesive; thus maximum principal stresses of the solid finite elements[2] are evaluated along the bonding at three different levels in

[2] The usage of averaged element stresses avoids stress singularities in the corner on the one hand. On the other hand, obtained stress levels are expected to be lower than directly on the interfaces. Please

bonding thickness direction: in the vicinity of the interface to steel, in the vicinity of the interface to glass and in the middle of the bonding. Figure 13 presents 2D results based on plain strain states for the baseline configuration with fully operational bonding starting from the end of the flanges– 0% bonding length – towards the symmetry axis in the front region – 100% bonding length. Please note that the corner of the bonding geometry is located at approximately 52% for all levels.

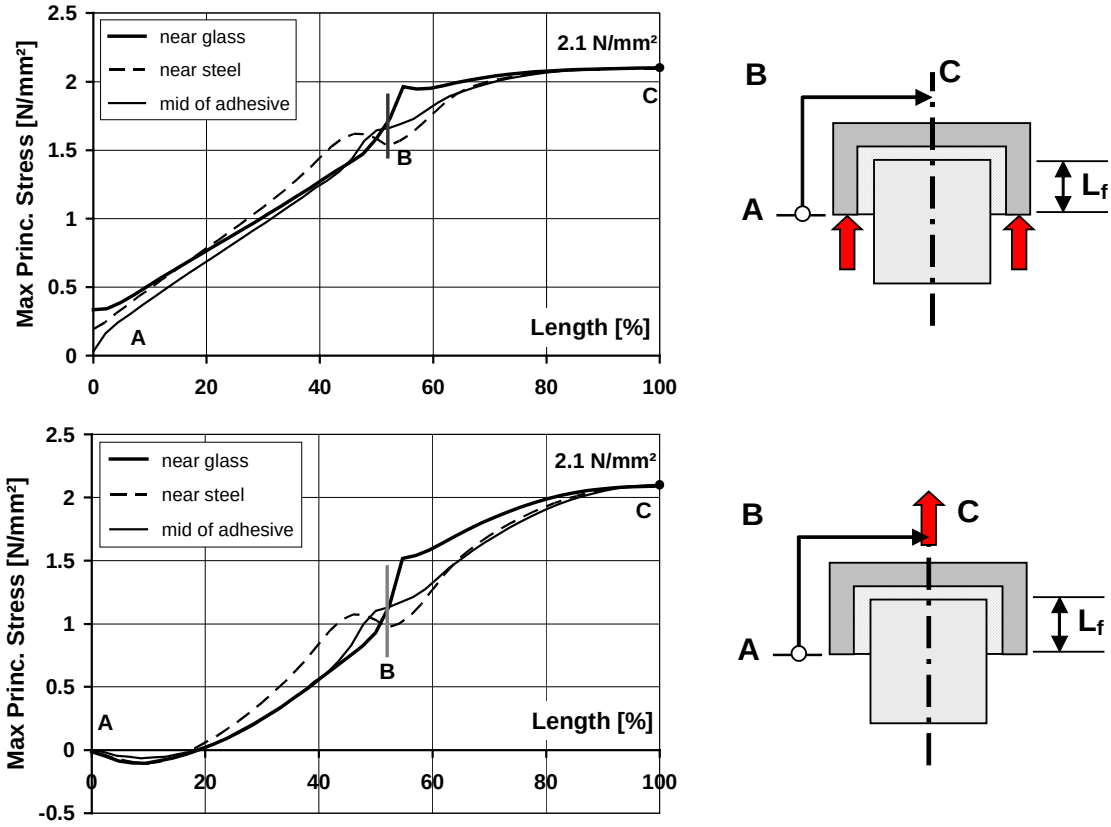

Figure 13 – *Maximum principal stress distribution in U-type bonding under various load introduction cases*

Two different load introduction configurations were analyzed – one with loads introduced at the flanges and one with loads introduced in the symmetry axis of the front region. The first configuration is often used for specimen testing while the later one represents a typical application case. The numerical models were loaded in such a way that a stress level of 2.1 N/mm^2 is achieved in the front region. The selection of this limit value is based on experimental findings.

The following conclusions can be drawn according to Figure 13:

- In the front region highest stress levels are experienced near the interface to glass.
- In the side region highest stress levels are mainly experienced near the interface to steel.

---

note that in the numerical model, the interfaces are geometric boundaries with stepped properties while in nature interfaces at least on the glass side show a different behavior on micro scale level.

- Stress levels in the side region are generally lower for loads introduced in the symmetry axis which is assumed to be more favorable for durability. It should be noted here that the difference in the stress results for the different load introduction points is due to flexibility of the PFC.
- Adjusting the loading to the limit stress level, the total load is different for both configurations – again a result related to the flexibility of the PFC.

As next step parameter studies were performed varying the length of the flange from 22 mm – which is the baseline value – down to 2 mm for the smallest flange. Figure 14 shows the stress levels only in the side region. In this case, an abscissa value of 0 mm corresponds to the free surface of the side region while the curves end for the different cases in the corners e.g. for 12 mm flange length at 12 mm on the glass side and 12 mm plus bonding thickness (5 mm) = 17 mm on the steel side etc. Figure 14 leads to the following conclusions:

- The difference of stress levels between glass side and steel side is small. Typically the glass side shows slightly increased stress values.
- The curves for 12 mm and 22 mm are very similar applying a shift of 10 mm which is the difference in the bonding geometry. Thus, it can be concluded that for these bonding geometries the loading inside is quite similar. The case of 2 mm flange length differs caused by interactions with the bonding corner.
- The curves for 12 mm and 22 mm show small stress levels at the free surface which is beneficial under durability aspects. For the 12 mm case stress levels immediately increase inside the bonding while for the 22 mm case, stress levels are even negative up to approximately 8 mm.
- If a representative penetration depth of aggressive environmental media is known in addition to a related allowable stress level, an optimized flange length can be approximated by horizontally shifting the 22 mm curve in such a way that it passes the allowable stress level at the length related to the penetration depth. The horizontal shift determines the enlarging or shortening of the flange for an optimized configuration.

Nevertheless, the size of the flange also affects other characteristics such as the failure characteristics in overload situation. In this case, additional design guidelines might have to be considered as well.

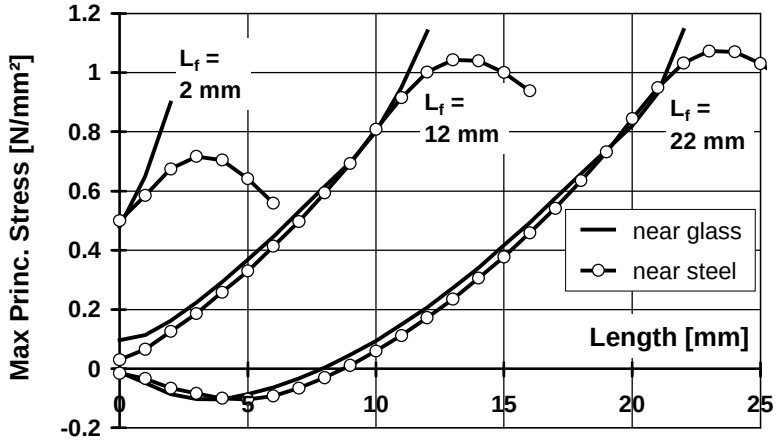

Figure 14 – *U-type bonding – maximum principal stress distribution for varying flange length*

T-type Bonding Geometries without and with Degradation

Similar to the U-type bonding, experiments have been performed for the T-type bonding with degradation (FRD) and without degradation (BSL) [6]. Figure 15 presents the results for a fully operative T-type bonding with a bonding degraded in the front region. The overall behavior shows significant similarities to the U-type bonding without and with failed front region. Again the front region leads on the one hand to high bonding stiffness and loads at the beginning of the test but on the other hand to early failure after 4 mm to 6 mm displacement. Afterwards, both curves of undegraded and degraded specimens are almost coincident indicating that loads are mainly transmitted by shear in case of these high displacements. These findings confirm that the conclusions of the failure start in the front region for U-type bonding geometries can also be applied to T-type bonding geometries. Furthermore, it is assumed that these statements do not hold only for U-type and T-type bonding geometries but for all bonding geometries with horizontal – i.e. perpendicular to the tension load aligned – front regions and vertical side regions i.e. parallel to the tension load. This assumption leads to the following conclusions:

- Bonding areas perpendicular to the tension loads and thus subjected to tension stresses lead to higher joint overall stiffness. The level of stiffness increase depends on the suppression of the lateral contraction.
- Due to the high stiffness of these bonding areas, local loads and stress levels will increase very fast with growing displacements. Thus, begin of failure will also start in this area.
- If bonding areas perpendicular to the tension loads start failing, load transfer will increasingly be established via shear by the bonding areas parallel to the applied tension loads.
- The maximum load capacity can be higher compared to the point of failure begin depending on bonding geometry, e.g. see Fig. 15. Thus, post-failure characteristics can be tuned by design means.

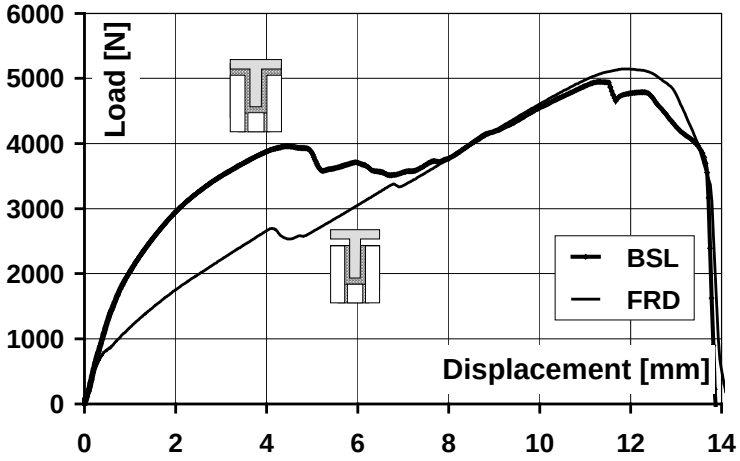

Figure 15 – *T-type bonding – test results [4]*

These four statements are fundamental concerning the general mechanical behavior of the joints. Taking additionally into account the durability aspect, it should be added that for favorable durability behavior the bonding areas perpendicular to the tensions loads should be encapsulated explained as in the following: In a similar manner as for the U-type bonding geometries, maximum principal stress levels are shown for T-type bonding geometries in Figure 16[3]. In contrast to the U-type bonding geometry, high stress levels are observed in the vicinity of the free bonding surface (label A) giving the T-type bonding geometry a very low ranking with respect to durability aspects. Furthermore, variation of the length of the flange does not significantly alter stress levels in the critical area for the fully operative bonding, see Figure 17. Results for two T-type bonding geometries are shown differing significantly in the length of the flange. Nevertheless, the stress levels at the free surface are quite similar. Of course, the behavior of these two different bonding geometries change in case of failure of the front region due to overloading or due to environmental attack of aggressive media. In this case, the size of the flange will define the remaining maximum load capacity and will lead to different characteristics.

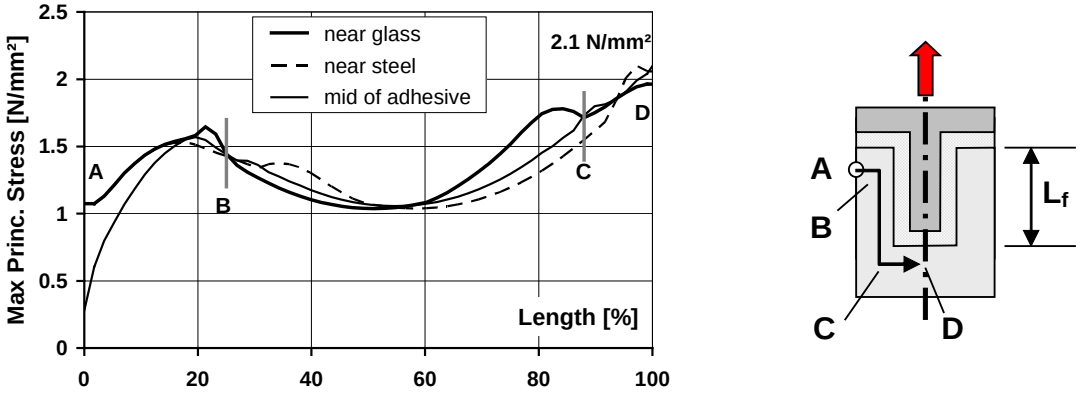

Figure 16 – *Maximum principal stress distribution in T-type bonding L_f = 35 mm*

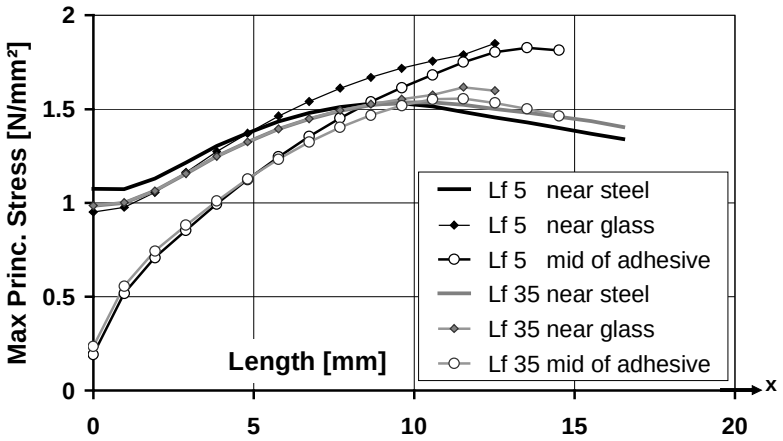

Figure 17 – *T-type bonding – maximum principal stress distribution for varying flange length*

[3] In this case only load introduction in the symmetry axis is considered.

Other Bonding Geometries of Interest: L and E

U-type and T-type bonding geometries can be understood as typical baseline geometries which can be used for derivation of other geometries. Examples might be here L- and E-type bonding geometries. The L-type bonding geometry can be interpreted as a modification of a U-type bonding geometry by eliminating one of the two side regions. Figure 18 presents experimental results for this bonding geometry confirming close relationship between U-type and L-type bonding geometries. The mechanical characteristics are very similar; thus a similar test campaign with degraded bonding was not taken into account. In the view of durability, L-type bonding geometries are assumed to be less favorable than U-type bonding geometries as one of the two free surfaces of the bonding geometry is located at the highly loaded front region. Depending on whether this side of the bonding is exposed to environmental attack the highly loaded front region might fail too fast due to these conditions. In this case, the size of the side region will determine the actual load capacity.

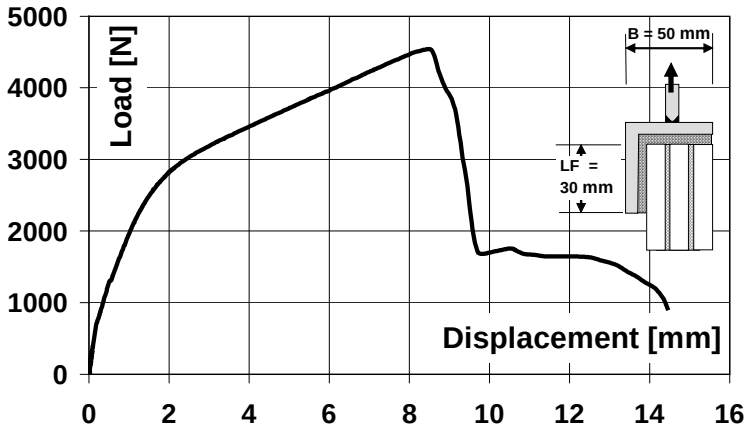

Figure 18 – *L-type bonding – test results [4]*

Figure 19 shows the stress levels for front and side region in the usual way confirming the above mentioned statements. While the stress distribution with respect to the side region is qualitatively in good agreement with the side region of the U-type bonding geometry, the stress distribution in the front region and especially at the free surface shows similarities with the front region of the T-type bonding geometry.

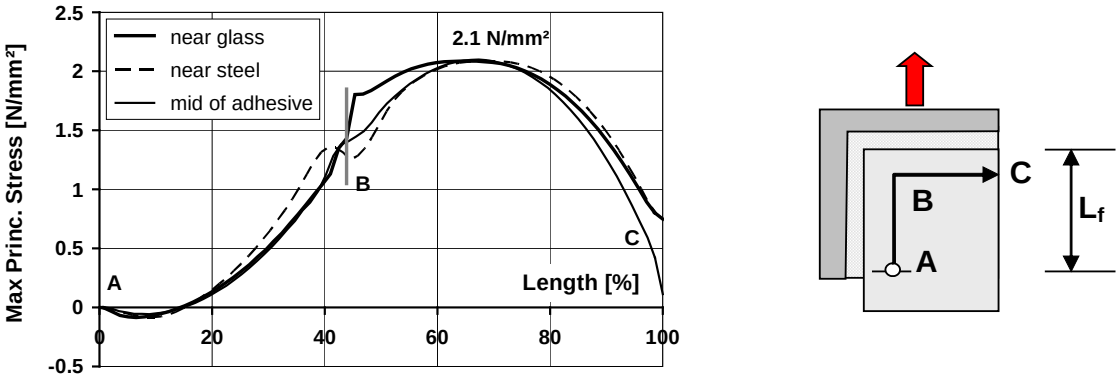

Figure 19 – *Maximum principal stress distribution in L-type bonding L_f = 30 mm*

Thus, it can be concluded that the free surface at the front region (label C) is the weak point with respect to durability in case both surfaces are exposed in the same way to the environment. Otherwise, it is recommended to put the side region of the L-type bonding geometry towards the more aggressive environment if possible.

The E-type bonding geometry can be understood as an extension of the U-type bonding geometry by adding the inner flange or as an extension of a T-type bonding geometry by adding two outside flanges. An application case can arise if the flange sizes should not exceed a certain geometric limit. For the E-type bonding geometry no experimental tests were performed. Nevertheless, it can be hypothesized that the mechanical behavior is similar to a composition of U-type bonding and T-type bonding. Under durability aspects, the E-type bonding geometry is assumed to correspond to U-type bonding geometries. These assumptions are underlined by Figure 20 showing the stress distributions for the E-type bonding geometry. The obtained stress distribution with respect to the outer side region is in qualitative agreement with the U-type bonding geometry while the inner flange loading is in qualitative agreement of the T-type bonding geometry.

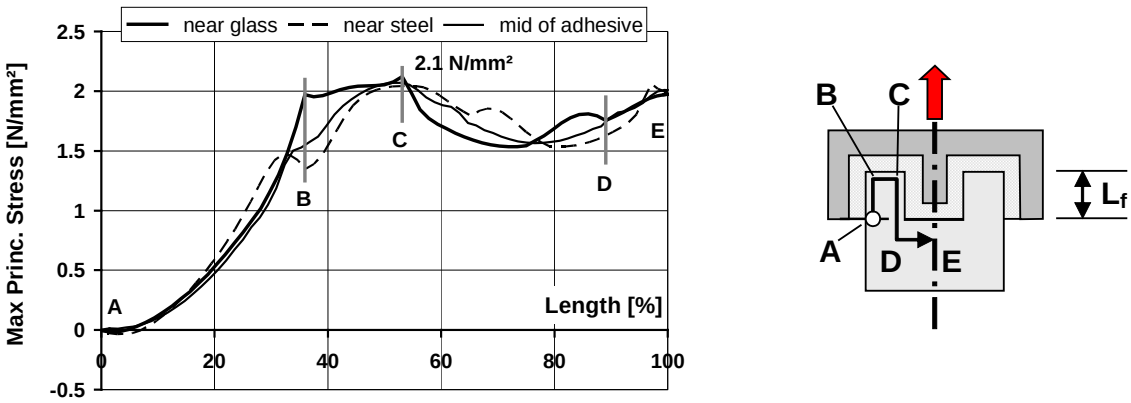

Figure 20 – *Maximum principal stress distribution in E-type bonding L_f = 22 mm*

Summary and Conclusions

This paper comprises two topics with high importance for structural joint durability. First, the joint material itself was in the middle of research activities. Tension and shear tests were performed for unaged and artificially aged specimens. Furthermore, corresponding tests took place for unaged specimens at different temperatures. Finally creep behavior was also tested in the frame of the tension tests. The experimental results were as follows:

- Regarding tension tests, aging leads to increased flexibility but no significant changes in strength are visible.
- Regarding shear tests, aging leads to increased flexibility and in addition to reduced strength.
- Regarding tension tests, increasing temperatures lead to increased flexibility but no clear trend is visible for strength.

- Regarding shear tests, increasing temperatures lead to increased flexibility and in addition to reduced strength.
- Regarding tension tests, creep does not show significant impact on flexibility and strength at higher loads.

Second different bonding geometries were analyzed with respect to durability issues. Working hypothesis is that the maximum principal stress level in the vicinity of the free surface of the bonding is a measure for durability. This assumption is based on the idea that the environmental impact of aggressive media and solar radiation is a function of depth below the free surface of the adhesive. Highest impact is related to the free surface while it is supposed that an attenuation of these effects appears with increasing distance from this surface. Regarding aggressive media, this assumption is guided by physical principles for diffusion into the adhesive while for radiation physical principles of absorption of the radiation have to be applied with respect to the adhesive. Although it is quite difficult to quantify the impact of these mechanisms on material strength by exact numbers, this idea allows to conclude design considerations for different bonding geometries such as U-type, T-type, L-type and E-type bonding geometries which were numerically and partially experimentally analyzed. Furthermore, the design considerations can be generalized to a class of bonding geometries with planes parallel and perpendicular to the critical tension load. Regarding durability it can be concluded that

- bonding geometries with all free surfaces only located at the end of a side region are ranked to show good durability properties in the context of applied stress. Examples are U-type bonding geometries and E-type bonding geometries.
- bonding geometries with at least one free surface located at a front region are ranked to show lower durability properties in the context of applied stress. Examples are T-type bonding geometries and L-type bonding geometries.

Please note that these statements hold for the fully operative bonding. The case of post-failure behavior is not treated in this paper with the exception of the presentation and discussion of experimental results for degraded bonding geometries in order to get increased physical insight.

Acknowledgement

The author would like to thank the customer – Erzdiözese München und Freising, Erzbischöfliches Baureferat – for unconditional support of the advanced design of the Herz-Jesu Church, Munich. Furthermore, the author would like to thank the Dow Corning company for their outstanding technical support provided during the design of the façade as well as in the related research phase.

References

[1] Hagl, A., *"Synthese aus Glas und Stahl: Die Herz-Jesu-Kirche München"*, Stahlbau 71, Heft 7, Ernst & Sohn Verlag, Berlin, Germany, 2002.

[2] Hagl, A., "Durability by Design: Load Carrying Silicone Bonding, Herz Jesu Church, Munich", *Durability of Building and Construction Sealants and Adhesives, ASTM STP 1453*, A.T. Wolf, Ed., ASTM International, West Conshohocken, PA, 2004.

[3] Kinloch, A. J. (Ed.), *"Durability of Structural Adhesives,"* Elsevier Applied Science Publishers Ltd., U.K., London, 1983.

[4] Fachhochschule München, FB02, "*Geklebte Verbindungen im Konstruktiven Glasbau"*, *Forschungsbericht*, abgeschlossenes BMBF Projekt, AIF-Nr.: 1755X04, 2007

[5] Hagl, A., "Understanding complex adhesive behaviour: Case study U-type bonding geometry", *Challenging Glass*, Bos Louter Veer, Eds., Delft University of Technology, May 2008

[6] Hagl, A., "*Klebungen bemessen – Tragende Verklebungen mit Silikon"*, Glas im konstruktiven Glasbau V, Germany, Muenchen, March 2007.